IOSR Journal of Mechanical and Civil Engineering (IOSR-JMCE)
e-ISSN: 2278-1684, p-ISSN: 2320-334X
PP 43-53
www.iosrjournals.org

Coupled wavelet-autoregression models for predicting monsoon flows for the Kosi River (India)

Rajeev R Sahay
(Civil Engineering Department, BIT Mesra, Patna Campus, India)

ABSTRACT: *Modeling monsoon flows are difficult as they are characterized by irregularly spaced spiky large events and sustained flows of varying duration. This paper investigates the efficiency of the couple wavelet-autoregression model (WR) for forecasting monsoon flows in a large river. WR combines two techniques, discrete wavelet transform (DWT) and autoregression (AR). DWT decomposes the original flow time series (OFTS) into its constituent wavelet components. Thereafter, a modified flow time series (MFTS) is obtained by removing the noise and recombining effective wavelet components. WR is an autoregression model implemented upon MFTS. The performance of WR models are evaluated using monsoon flows of the Kosi River at Barahchhetra gauge-site. During monsoon (June to September), the Kosi carries large flows submerging a large part of Bihar State of India. The results of the study show that the proposed WR models forecast river flows more reliably than autoregression (AR) and artificial neural network (ANN) models, developed for the comparison purpose. The best performing WR model, with three previous days' flows as inputs, predicted the Kosi flows with 90.4% accuracy, while the best ANN and AR models forecasted them with only 87.8% and 82.2% accuracies respectively. In addition, WR models predicted relatively reasonable estimates for the extreme flows, showing little bias for under- or overprediction.*

Keywords - *Artificial neural network, autoregression, discrete wavelet transform, floods, Kosi, India*

1. Introduction

Forecasting river flows constitutes major input information for issues such as water resources planning and management, water diversion, flood fighting and environment sustainability. Most of the previous works on river flow forecasting reported in literature can broadly be kept into two major groups, conceptual and data-based. The conceptual models, despite adequately describing the hydrological processes based on physical laws, are not very popular as they require intensive data and complicated differential equations for their implementation. On comparison, data-based models have recently gained popularity in hydrological applications due to their rapid development times, fewer data requirement and ease of real-time implementation [1]. These models establish input-output relationships without accounting explicitly to the physical laws which govern the hydrological processes. Autoregression and artificial neural network are very popular data-based forecasting techniques; however, autoregression models are found unsuitable for handling data with transitory characteristics such as drifts, trends and abrupt changes. Though, artificial neural network has the ability to learn relationship between non-stationary inputs and outputs [2], its optimal structure is hard to determine. In addition, the surface of the objective function of a neural network is non-convex and contains multiple local optima where the network solution gets easily trapped.

In the last decades, the wavelet transform has become a useful data-based technique for analyzing variations, periodicities and trends in a time series. [3] used discrete wavelet transform for classifying streamflows into distinct hydro-climatic categories. [4] applied wavelet methods to model rainfall and runoff measured at different sampling rates, from daily to half-hourly. [5] used DWT for updating wavelet coefficients of a unit hydrograph and convoluted these coefficients with effective rainfall for predicting one-step-ahead runoff in a Taiwanese Basin. [6] used wavelet analysis to identify variability in annual flows in Canadian Rivers. [7] implemented wavelet regression for modeling daily flow rates of Arkansas River at Syracuse and Kendail gauge stations in USA. [8] successfully used DWT for determining possible trends in the annual precipitation in Turkey. [9] developed wavelet network model to forecast seasonal mean discharge, mean daily discharge and annual mean discharge for Three Gorges dam in Yangtze River of China. [10] developed a wavelet regression model as an alternative to neural network for monthly streamflow forecasting. [11] developed a hybrid model of wavelet and artificial neural network to predict sediment load in rivers. [12] developed a combined model of generalized regression neural network and wavelet for monthly streamflow prediction. [13] developed continuous wavelet transform to investigate the variability of lake levels in four lakes in the Great Lakes Region. [14] developed a wavelet-ANN conjunction model to predict the monthly concentration of diffuse pollution in a stream. [15] developed wavelet regression models for forecasting river stages and found them

superior to ANN and AR models. [16] developed wavelet-ANN and wavelet-support vector machine models for reservoir inflow prediction.

The foregoing discussion suggests a time series when pre-processed by wavelet transform improves the accuracy of a forecasting tool. This is because in dissociation of a time series by wavelet transform, the noise component can be easily identified and removed. In the present study, the efficiency of a coupled model of discrete wavelet transform and autoregression was investigated for predicting monsoon flows. Predicting monsoon flows poses greater challenge as their magnitude and variation are very high. Autoregression was selected as a forecasting tool as it is simple to develop and widely used for hydrologic modeling. We also included ANN as it is well suited for modeling nonlinear, nonstationary and nongaussian processes like those encountered in hydrological contexts. A case study of the developed models was made to the Kosi River in India. The Kosi, also nicknamed 'Sorrow of Bihar', has a long history of flooding and meandering. Accurate flow forecasting should go a long way in taking up flood fighting and water diversion measures.

2. Adopted Methodologies

The following subsections describe the methodologies adopted in the present work:

2.1 Artificial Neural Network

ANN, first introduced by [17] as a mathematical structure capable of representing the complex nonlinear processes that relate the inputs to the outputs of a system, is inspired by the neural structure of our brain. It can be characterized as massively parallel interconnections of simple neurons that function as a collective system. This ability of ANNs to capture relationships from given patterns has enabled them to be employed in various hydraulic and hydrologic problems such as rainfall-runoff modeling, stream flow prediction, ground water modeling, water quality, water management, precipitation forecasting, time-series analysis, reservoir operations and other hydrologic applications. A review of ANN applications in hydrology is presented in [18].

The most widely used ANN structures are three-layer feed forward networks. A typical three-layer feed forward ANN has g, n, and m nodes or neurons in the input, hidden, and output layers, respectively. Neurons of a layer are connected to every neuron of the succeeding layer but are not connected among themselves. The parameters associated with each of the connections nodes, called weights, signify relative importance of the connections. All connections are feed forward, i.e., they allow information transfer only from an earlier layer to the next consecutive layers. Each node *j* receives incoming signals from every node *i*, (β_i), in the previous layer magnified by the weight of the connection (θ_{ji}). The effective incoming signal (α_j) to node *j* is the weighted sum of all the incoming signals plus a bias (λ_j), i.e.

$$\alpha_j = \sum \theta_{ji}\, \beta_i + \lambda_j \qquad (1)$$

The effective incoming signal, α_j, is passed through a transfer function *g* (also called an activation function) to produce the outgoing signal (y_j) of the node *j*. In this study, sigmoid nonlinear transfer function has been used in the hidden as well as the output layers, i.e.

$$y_j = g(\alpha_j) = \frac{1}{1+e^{-\alpha_j}} \qquad (2)$$

In the above equation, the incoming signal α_j can vary on the range (-∞, ∞), and the output signal y_j on the range (0, 1). Because of sigmoid transfer function in the present study, data variables are normalized onto range (0, 1) before applying the ANN methodology. To determine the set of optimal weights and biases, the created ANN network is first trained using known inputs and outputs in some ordered manner, adjusting the interconnection weights and biases until the desired outputs are achieved. The Levenberg-Marquardt training algorithm [19] was employed in this study. The algorithm assumes that the underlying function modeled by ANN is linear. The number of nodes in the hidden layer is determined by trial and error. In the present work, ANNs with range of 1-12 hidden nodes were tried on the training datasets. The ANN producing the best performance, i.e., the minimum root mean square error on the verification dataset was selected for forecasting the Kosi flows. [20] has given a good illustration of the working of ANN.

2.2 Autoregression

It has been observed that the values of a discharge series of a river at a particular time-step are highly related with the values that precede and succeed them; therefore, the system can generate internal dynamics between inputs and outputs. A P^{th} order autocorrelation, i.e., AR (*P*), which refers to the size of the correlation between values in a time series that are p periods apart is given by

$$x_i = \sum_{i=1}^{P} \theta_i \, x_{i-1} + \varepsilon_t \quad (3)$$

where θ_i are the autoregression coefficients, x_i is the time series under investigation and *P* is the order (length) of the AR model. The residue term, ε_t, is assumed to be the Gaussian white noise. *P* is generally much less than the data length of the series. Thus, in autoregression, the current discharge can be estimated by a linear weighted sum of previous discharges in the series. The weights are the autoregression coefficients which are normally estimated using the least square method based on Yule-Walker equation. AR has been a popular method in a wide spectrum of engineering problems. Some of the recent applications of AR in water resources engineering may be found in [21] and [22].

2.3 Discrete Wavelet Transform

Wavelet analysis is a windowing technique in which signals are broken up into shifted and scaled versions of an original wavelet, called as the mother wavelet (Fig. 1). A wavelet is a waveform of effectively limited duration that has an average value of zero. On comparison, sine waves, which are the building blocks of Fourier analysis, have unlimited duration extending from minus infinity to plus infinity. Also, wavelets are irregular and asymmetric unlike sinusoids which are smooth and predictable. These attributes make wavelets suitable for analyzing signals with transitory characteristics such as drifts, trends and abrupt changes.

A wavelet transform involves convolving the signal against particular instances of a wavelet at various time scales and positions. To perform these convolutions at every position and scale, a mathematical technique called continuous wavelet transform (CWT) is implemented. CWT of the time series, *f (t)*, with respect to a mother wavelet, $\varphi(t)$, is defined as the sum over all time of the signal multiplied by the scaled and shifted version of the mother wavelet $\varphi(t)$:

$$T_{a,b} = \frac{1}{\sqrt{a}} \int_{-\infty}^{\infty} f(t) \, \varphi^*\left(\frac{t-b}{a}\right) dt \quad (4)$$

The results of CWT are many wavelet coefficients. They are functions of scale and position and give a measure of correlation between the scaled and shifted wavelet and the original signal. The conjugate wavelet basis functions, $\varphi^*\left(\frac{t-b}{a}\right)$, are derived from a common mother wavelet function $\varphi_{(0,0)}(t)$ by scaling (or dilating) it by a and translating it by b :

$$\varphi_{a,b}(t) = 2^{-a/2} \, \varphi_{0,0} \, (2^{-a} t - b) \quad (5)$$

Determining wavelet coefficients at every possible scale is an enormous task and time consuming. Moreover, actual flow data are measured at specific time intervals and are discrete in nature. DWT is found more suitable in analyzing such time series. DWT normally uses dyadic scheme of wavelet decomposition where alternate scale and position is adopted for calculating transform coefficients, reducing the computational burden. For a discrete time series x_i with integer time steps, DWT in dyadic decomposition scheme is defined as

$$T_{m,n} = 2^{-m/2} \sum_{i=0}^{N-1} x_i \, \varphi(2^{-m} i - n) \quad (6)$$

where, $T_{m,n}$ is the wavelet coefficient for scale $a=2^m$, and location $b=2^m$ n, m and n being positive integers. N is the data length of the time series and is an integer power of 2, i.e., $N=2^M$. This gives the ranges of m and n as $0 < n < 2^{M-m}-1$ and $1 < m < M$, respectively. The original time series may be reconstructed employing inverse discrete transform:

$$x_i = \bar{T} + \sum_{m=1}^{M} \sum_{n=0}^{2^{M-m}-1} T_{m,n} 2^{-m/2} \varphi(2^{-m} i - n) \quad (7)$$

or, in a simple format as:

$$x_i = \bar{T}(t) + \sum_{m=1}^{M} W_m(t) \quad (8)$$

where, $\bar{T}(t)$ is called approximation sub-time series (denoted by A in this study) at level M and $W_m(t)$ are details sub-time series (denoted by D in this study) at levels $m = 1,2,\ldots M$.

[23] devised an efficient way of estimating DWT coefficients at every subset of scale and position utilizing filters. The process consists of a number of successive filtering steps in which the time series is decomposed into 'approximation' and 'details' sub-time series/wavelet components. Approximation wavelet components represent the slowly changing coarse features of a time series and are obtained by correlating stretched version (low-frequency and high-scale) of the mother wavelet with the original time series, while detail coefficients signify rapidly changing features of the time series and are obtained by correlating compressed version of the mother wavelet (high-frequency and low-scale) with the original time series. The decomposition process can be iterated, with successive decomposition of approximation wavelet components so as to break the original signal into many lower resolution components (Fig. 2).

2.4 Wavelet-Autoregression

A conjunction model, WR, is formed by combining DWT and AR. DWT decomposes OFTS into its wavelet components on suitable decomposition levels. With the increase in decomposition level, fluctuation reduces and we see a smooth series at the third resolution level. This can be observed from Fig. 3 which shows the decomposed wavelet components of the Kosi River on three decomposition levels. For accurate and reliable modeling, it is important to remove the noise components from a time series. With this objective, a correlation study between the sub-time series and the original time series was carried out (Table 1). In Table 1, Di_{t-1} denotes the sub-time series on i^{th} resolution level at time t-1 and Q_t denotes the original time series at time t. As can be seen, the coefficient of correlation increased with increase in resolution level. MFTS is developed combining sub-time series components D_2, D_3 and A_3. Thus, MFTS is the denoised version of OFTS and WR is essentially an autoregression model that uses MFTS hydrograph for input. The working structure of WR model is shown in Fig. 4.

3. Model Implementation

Three models each of WR (e.g., WR1, WR2 and WR3), AR (e.g., AR1, AR2 and AR3) and ANN (e.g., ANN1, ANN2 and ANN3) were developed. Table 3 shows the structures and inputs for the developed models. WR3, for example, had q_{t-1}, q_{t-2} and q_{t-3}, i.e., 1-day-, 2-days- and 3-days-before flows respectively from MFTS for inputs, while inputs for AR3 and ANN3 consisted of Q_{t-1}, Q_{t-2} and Q_{t-3}, i.e., 1-day-, 2-days- and 3-days-before flows respectively from OFTS. The desired output in all models was the current flow, i.e., Q_t. For performance evaluation, prediction by WR, AR and ANN models are compared using statistical indices like coefficient of correlation (CC), root mean square error (RMSE), discrepancy ratio (DR) and % accuracy, which are defined as

$$CC = \frac{\sum_{i=1}^{N} Q_p Q_m - \sum_{i=1}^{N} Q_p \sum_{i=1}^{N} Q_m}{N S_p S_m} \quad (9)$$

$$RMSE = \sqrt{\frac{\sum_{i=1}^{N} (Q_p - Q_m)^2}{N}} \quad (10)$$

$$DR = log \frac{Q_p}{Q_m} \quad (11)$$

$$\% \, Accuracy = \frac{100\,N'}{N} \quad (12)$$

where Q_p and Q_m are the predicted and measured flow rates in the river respectively; S_p and S_m are standard deviations in the predicted and measured flows, respectively; N is the total number of observations and N' is the number of predictions lying between 80% and 120% of the measured values (i.e., DR value lying between -0.1 and 0.1). From Eq. (11), DR=0 suggests exact match between the measured and the predicted flows, otherwise, there is either underprediction [DR<0 i.e., $Q_p < Q_m$] or overprediction [DR>0, i.e., $Q_p > Q_m$].

3.1 Study Area

The Kosi River, a transnational river, originates at an altitude of over 7000 m above MSL in the Himalayas. Its upper catchment lies in Nepal and Tibet. Mount Everest, the highest peak in the world, lies in its catchment. Its basin is surrounded by the ridges separating it from the Brahmaputra in the north, the Gandaki in the west, the Mahananda in the east and the Ganga in the south. The Kamla, the Baghmati (Kareh) and the Budhi Gandak are major tributaries of the Kosi in India, besides many other minor tributaries. Through Nepal, the Kosi enters the Indian Territory near Hanuman Nagar in Bihar State of India where it flows through a length of 260 km before meeting the Ganga River in Katihar District of Bihar. The Kosi River drains a total catchment area of 74030 sq km, out of which only 11410 sq km lies in India and the rest in Tibet and Nepal. The catchment map of the Kosi in India along with the other adjoining river basins is shown in Fig. 5. Flooding in the Kosi Basin is a recurrent event. Any heavy downpour in its upper catchment rushes toward the Indian Territory which takes away many lives and causes damage to infrastructure, agriculture and industrial production. In the year 2008, a breach in the Kosi embankment caused the biggest ever flood disaster in India that spread to over 0.4 million hectares of land affecting over three million people. Because of steep gradient and loose nature of soil in its upper catchment, the Kosi carries heavy silt and has tendency to move sideways. In the last 200 years, the river has moved laterally by about 170 km. To confine the river and to control the flood damages, long embankments measuring 798 km on both sides of the river are constructed. Although, the embankments have confined the lateral shift of the river to a large extent, frequent breaches and over-toppings of the embankment have made flooding a perpetual challenge in the area. The hydro-meteorological data is collected in the region through a network of gauge and discharge stations on the various North-Bihar Rivers by government agencies like Central Water Commission and Water Resources Department.

For deriving and verifying the developed models, the Kosi's flow data for five years at Barahchhetra gauge-site for the monsoon period were used. While 492 daily flow data for the years 2001-04 were used for deriving the models, 241 daily flow data for the years 2006-07 were utilized for verifying the models. Due to unavailability of the data, the year 2005 could not be included in this study. Table 2 summarizes the statistical information on the observed flow data of the Kosi River for the monsoon period.

To derive WR models, first, OFTS is decomposed into its sub-time series by DWT on suitable resolution levels. [24] suggested log (n) resolution levels, where n is the length of the time series. In our study, 492 daily data were used for deriving the models, hence three decomposition levels were considered sufficient. The sub-time series, i.e., D1, D2 and D3 represent detail sub-time series corresponding to 2-, 4- and 8-days' scale or periodicity respectively, while A3 represents approximation sub-time series of 8-days' scale. According to [2], D1 components make forecasting time series difficult as it has the lowest correlation and may contain the noisy part of the original time series, therefore, D1 was excluded and a modified flow time series was obtained by adding D2, D3 and A3 sub-time series. The selection of a suitable mother wavelet in decomposing the time series is a critical issue as the efficiency of WR models is also dependent on it. Widely used wavelets in hydrological modeling are haar, db3, db6, db10, sym9, coif5, bior6.8, rbio6.8 and dmey. In this study, db6 was found the most suitable mother wavelet for simulating the Kosi River flows.

4. Results and Discussion

The performance of the developed models was evaluated for forecasting the Kosi flows at Barahchhetra gauge-site for the monsoon period. Table 3 summarizes the performance of the models for the derivation as well as the verification datasets. It shows WR models performing better than AR and ANN models. Even the simplest wavelet regression model, WR1, with just one input, predicts the flows with accuracy as high as 89.6% for the verification dataset, where % accuracy is defined as the percentage of predicted values lying between 80% and 120% of the measured values. On comparison, ANN1 and AR1 have the accuracies of only 84.7% and 81.3%

respectively. The other performance indicators, CC and RMSE are also found superior for WR1 than for ANN1 and AR1. For the derivation dataset also, WR1 performs better than AR1 and ANN1. Another input, q_{t-1}/Q_{t-1} was added to WR2, AR2 and ANN2 to see the effect of an additional input on the performance of the models. As can be seen from Tables 3, the performance of the wavelet and the neural network models improves with better CC, RMSE and % accuracy parameters, however, there is hardly any improvement in autoregresson model. Models WR3, ANN3 and AR3 were developed with three antecedent days' flows as inputs. As can be observed from Table 3, their performance is only marginally better than the previous models. In fact, there is no improvement in AR model for the verification dataset while RMSE slightly decreases from 502 m^3/s to 501 m^3/s for the derivation dataset. Also, the performance of ANN3 deteriorates for the derivation dataset as RMSE increases from 483 m^3/s to 485 m^3/s, however, for the verification dataset, it decreases from 593 m^3/s to 590 m^3/s.

Of all the developed models, WR3 (Eq. 13) predicts the Kosi flows best with CC of 0.934, RMSE of 544 m^3/s and %accuracy of 90.4 for the verification dataset. For the derivation dataset also, its performance is better than AR3 (Eq. 14) and ANN3, which are found the best performing models in autoregression and artificial neural network categories. WR3 successfully predicts the highest three flows of 9149 m^3/s, 8518 m^3/s and 8395 m^3/s from the whole dataset as 8674 m^3/s, 7570 m^3/s, and 8252 m^3/s, respectively. On comparison, prediction for the highest three flows by AR3 and ANN3 are 5597 m^3/s, 6855 m^3/s and 6276 m^3/s respectively, and 7948 m^3/s, 8135 m^3/s and 7659 m^3/s respectively. The prediction by WR3 for the low discharges also seems to be in good agreement to the measured data, estimating the lowest three flows of 853 m^3/s, 878 m^3/s and 993 m^3/s as 921 m^3/s, 1115 m^3/s, and 951 m^3/s respectively, while AR3 and ANN3 predict them as 1126 m^3/s, 1219 m^3/s and 1098 m^3/s respectively, and 1055 m^3/s, 1166 m^3/s and 1026 m^3/s respectively. This implies that WR3 captured the input-output pattern well even for the extreme flows.

$$Q_t = 129 + 1.423\, q_{t-1} - 0.386\, q_{t-2} - 0.083\, q_{t-3} \quad (13)$$

$$Q_t = 324 + 0.87\, Q_{t-1} + 0.02\, Q_{t-2} + 0.015\, Q_{t-3} \quad (14)$$

Fig. 6 shows the predicted and measured flows of the Kosi River for the verification dataset by WR3, AR3 and ANN3. It shows WR3 to have the least deviation between the measured and predicted Kosi flows. Another performance indicator of a model, the DR range, which shows proximity between the predicted and the original flow time series, for WR3, is -0.20 to 0.16, showing little bias for underprediction. However, models AR3 and ANN3 show greater positive and negative skewnesses respectively with DR ranges -0.25 to 0.28 and -0.24 and 0.22 respectively. Fig. 7 shows percentage of predicted values by different models falling into different discrepancy brackets. It shows an even distribution for the predictions by WR3 with 97% of predictions lying between DR range of -0.2 and 0.2, the best among all models.

Though, the above discussion suggests WR models efficient in monsoon flow forecasting, it should be understood that the present study used daily flow data for only 5 years which may not be representative of complexity of a large river system like the Kosi. Furthermore, the developed models are location and period specific; hence, these models are sensitive and may have significant phase problems if made to forecast flows for non-monsoon periods, as the causes of floods are different at other points of the year. For example, monsoon rainfall brings floods in North Bihar Rivers during June–Sept, while glacier-melt contributes significantly to their flows during Jan-May. Therefore, the forecasting models should be developed for a specific period by considering the data for that period only.

5. Conclusions

A coupled method, wavelet regression, was developed combining discrete wavelet transform and autoregression to predict monsoon flows in a large river. Monsoon flows are irregular high flows with large variations, modeling of which poses great challenge. Three WR models were developed and a practical application of the developed models was made to the Kosi River at Barahchhetra gauge site. The performance of WR models was evaluated along with AR and ANN models, developed for the comparison purpose. Based on several statistical indices like coefficient of correlation, root mean square error and discrepancy ratio, it was concluded that WR models predict flows with greater accuracy than AR and ANN models. The best performing WR model, with the last 3 days' antecedent flow rates as inputs, predicted the current Kosi flows with 90.4% accuracy while the best performing AR and ANN models predicted these flows with only 87.8% and 82.2% accuracies respectively.

Acknowledgement

The authors acknowledge the support rendered by All India Council of Technical Education, New Delhi, India (F.N.: 8023/BOR/RID/RPS-45/2007-8) and University Grants Commission, New Delhi, India (F.N. 33-482/2007).

References:

[1] J. F. Adamowski, River flow forecasting using wavelet and cross-wavelet transform models, *Hydrological Processes*, *22*, 2008, 4877-4891.
[2] O. Kisi, and J. Shiri, Discussion on Precipitation Forecasting Using Wavelet-Genetic Programming and Wavelet-Neuro-Fuzzy Conjunction Models." *Water Resources Management*, 2012, DOI 10.1007/s 11269-012-0060-y.
[3] L. C. Smith, D. L. Turcotte, and B. Isacks, Stream flow characterization and feature detection using a discrete wavelet transform, *Hydrological Processes*, 12, 1998, 233–249.
[4] D. Labat, R. Ababou, and A. Mangin, Rainfall-runoff relation for karstic spring, part 2. Continuous wavelet and discrete orthogonal multi resolution analyses, *Journal of Hydrology*, 238, 2000, 149-178.
[5] C.M. Chou, and R.Y. Wang, On-line estimation of unit hydrographs using the wavelet-based LMS algorithm, *Hydrological Science Journal*, 47, 2002, 721–738.
[6] P. Coulibaly, and H. D. Burn, Wavelet analysis of variability in annual Canadian streamflows, *Water Resource Research*, 40, 2004, W03105, doi.10.1029/2003WR002667.
[7] M. Kucuk, and N. Agiralioglu, Wavelet regression techniques for streamflow predictions, *Journal of Applied Statistics*, 33, 2006, 943–960.
[8] T. Partal, and M. Kucuk, Long-term trend analysis using discrete wavelet components of annual precipitations measurements in Marmara region (Turkey), *Physics and Chemistry of the Earth*, 31, 2006, 1189-1200.
[9] H. C. Zhou, Y. Peng, G. H. Liang, The research of monthly discharge predictor-corrector model based on wavelet decomposition, *Water Resources Management*, 22, 2008, 217–227.
[10] O. Kisi, Wavelet regression model as an alternative to neural networks for monthly streamflow forecasting, *Hydrological Processes*, 23, 2009, 3583–3597.
[11] T. Rajaee, S. A. Mirbagheri, V. Nourani, and A. Alikhani, Prediction of daily suspended sediment load using wavelet and neuro-fuzzy combined model, *International Journal of Environmental Science and Technology*, 7, (2010). 93-110.
[12] O. Kisi, Wavelet Regression Model as an Alternative to Neural Networks for River Stage Forecasting, *Water Resource Management*, 25, 2011, 579–600.
[13] T. M. Cenzig, Periodic structures of great lakes levels using wavelet analysis, *Journal of Hydrology and Hydromechanics*, *59*, 2011, 24–35.
[14] R. M. Singh, Wavelet-Ann Model For Diffuse Pollution Prediction In Streams, *ISH Journal of Hydraulic Engineering*, 17(1), 2011, 1-11.
[15] R. R. Sahay, and V. Sehgal, Wavelet regression models for predicting flood stages in rivers. a case study in Eastern India, *Journal of Flood Risk Management*, 6, 2013, 146-155.
[16] U. Okkan, and Z. A. Serbes, The combined use of wavelet transform and black box models in reservoir inflow modelling, *Journal of Hydrology & Hydromechanics*, 61, 2013, 112–119.
[17] W. S. Mcculloch, and W. H. Pitts, A logical calculus of the ideas immanent in nervous activity, *Bulletin of Mathematical Biophysics*, 5, 1943, 115-133.
[18] ASCE Task Committee on Application of Artificial Neural Networks in Hydrology Artificial Neural Networks in hydrology- II: hydrologic applications, *Journal of Hydrologic Engineering*, *5*, 2000b, 124-137.
[19] A. J. Shepherd, *Second-order methods for neural networks* (Springer, New York, 1997).
[20] S. Haykin, *Neural networks, a comprehensive foundation*. Macmillan College Publishing Co. New York, 1994.
[21] M. Leclerc, and T. B. M. J. Ouarda, Non-stationary regional flood frequency analysis at ungauged sites, *Journal of Hydrology*, 343, 2007, 254–265.
[22] G. B. Sahoo, S. G. Schladow, and J. E. Reuter, Forecasting stream water temperature using regression analysis, artificial neural network, and chaotic non-linear dynamic models, *Journal of Hydrology*, 378, 2009, 325-342.
[23] S. G. Mallat, A theory for multi resolution signal decomposition: the wavelet representation, *IEEE Transactions on Pattern Analysis and Machine Intelligence*, 11, 1989, 674–693.
[24] W. Wang, and J. Ding, Wavelet network model and its application to the prediction of the hydrology, *Nature and Science*, 1, 2003, 67–71.
[25] FMIS, *Flood management information system* (Water Resources Department, Government of Bihar, India, 2013).

Figure 1. Decomposition of time series into wavelets

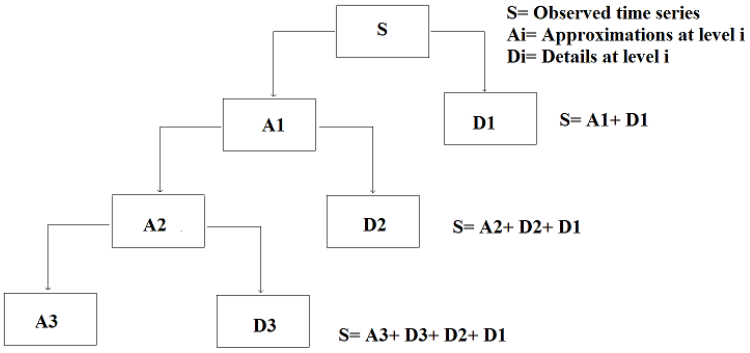

Figure 2. Decomposition of time series into approximations and details

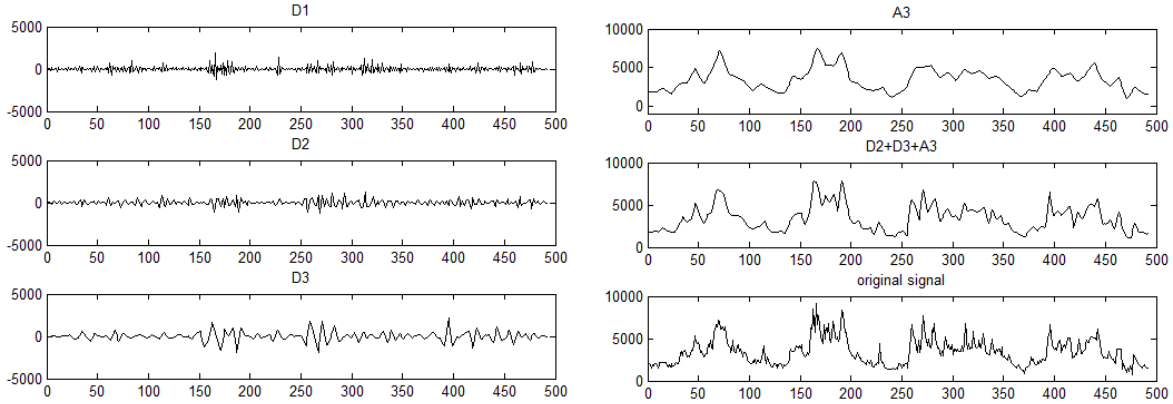

Figure 3. Decomposition of the Kosi flow series into wavelet components (derivation dataset)

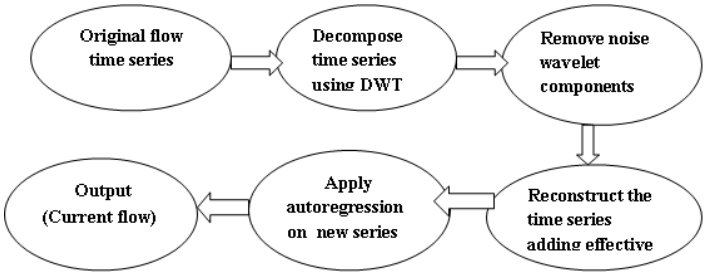

Figure 4. Working structure of WR model

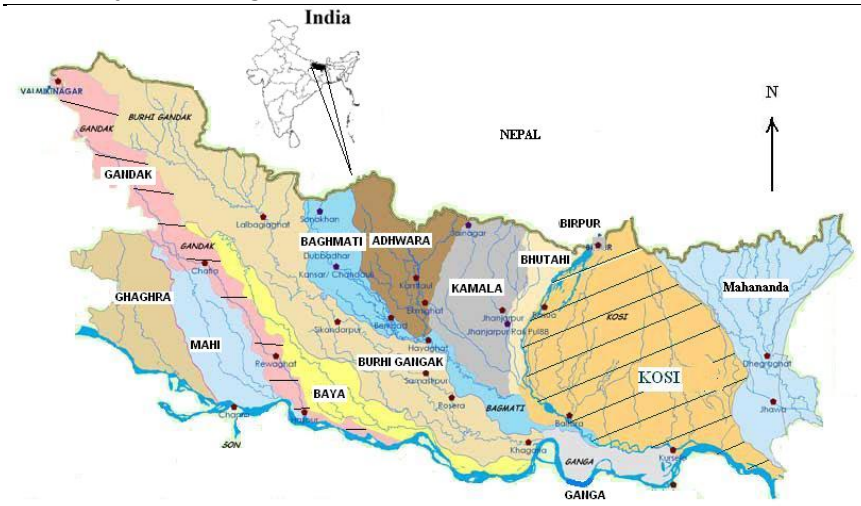

Figure 5. Basin map of the Kosi and the adjoining rivers (FMIS 2013)

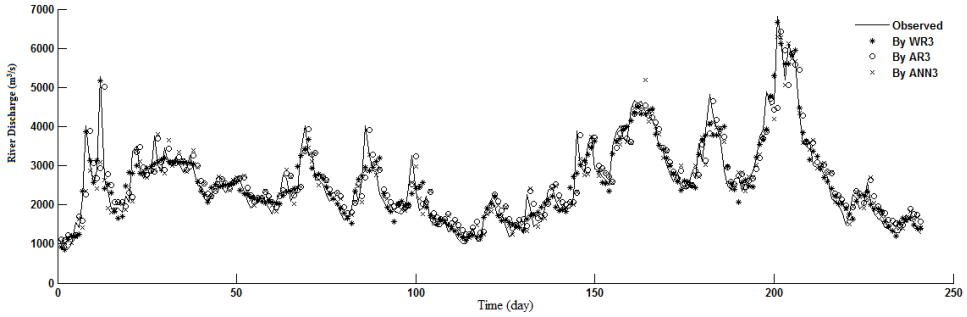

Figure 6. Observed and predicted flows in the Kosi River (verification dataset)

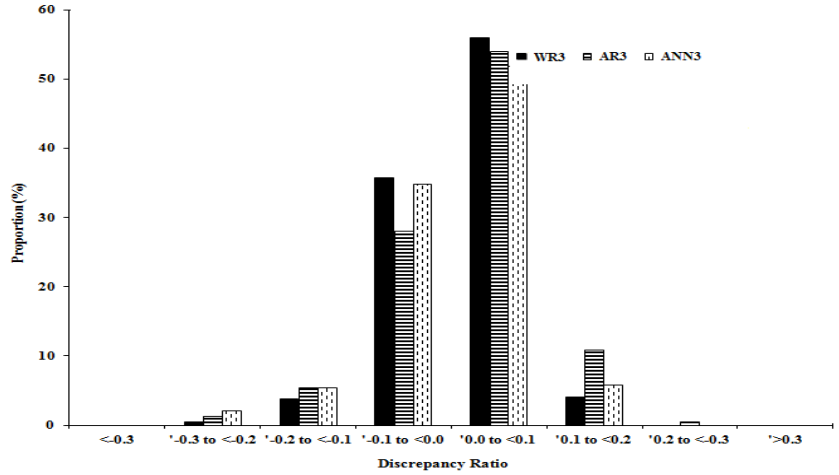

Figure 7. Comparison of discrepancy ratio

Table 1: CC between the wavelet components and the flow time series of the Kosi at Barahchhetra

Wavelet component	Di_{t-1}/Q_t	Di_{t-2}/Q_t	Di_{t-3}/Q_t	Di_{t-4}/Q_t	Avg.
$Di_{(i=1)}$	-0.053	-0.073	0.028	0.058	-0.010
$Di_{(i=2)}$	0.083	0.061	0.131	-0.101	0.044
$Di_{(i=3)}$	0.436	0.253	0.121	-0.043	0.192
Wavelet component	A_3/Q_t	A_3/Q_t	A_3/Q_t	A_3/Q_t	Avg.
A_3	0.761	0.673	0.575	0.573	0.646

Table 2. Statistical characteristics of the Kosi's monsoon flows at Barahchhetra

Data set	Mean (m^3/s)	Minimum (m^3/s)	Maximum (m^3/s)	Standard Deviation (m^3/s)	Skewness
Derivation (2001-04)	3437	764	9149	1530	1.0
Verification (2006-07)	2981	853	6826	1053	1.0
Whole	3136	764	9149	1453	1.0

Table 3. Performance indices of the developed models

Input variables	Model	Derivation dataset		Verification dataset			
		CC	RMSE (m^3/s)	CC	RMSE (m^3/s)	DR Range	Accuracy (%)
q_{t-1}	WR1	0.923	392	0.928	570	-0.22 to 0.17	89.6
Q_{t-1}	AR1	0.900	503	0.881	664	- 0.25 to 0.28	81.3
	ANN1	0.916	478	0.907	616	- 0.24 to 0.26	84.7
q_{t-1} & q_{t-2}	WR2	0.935	373	0.934	545	- 0.20 to 0.16	90.2
Q_{t-1} & Q_{t-2}	AR2	0.901	502	0.882	664	- 0.26 to 0.28	82.2
	ANN2	0.916	483	0.915	593	- 0.24 to 0.22	87.0
q_{t-1}, q_{t-2} & q_{t-3}	WR3	0.935	373	0.934	544	- 0.20 to 0.16	90.4
Q_{t-1}, Q_{t-2} & Q_{t-3}	AR3	0.901	501	0.882	664	- 0.25 to 0.28	82.2
	ANN3	0.921	485	0.919	590	- 0.24 to 0.22	87.8

Note: Q_{t-n} and q_{t-n} are n-day antecedent flows for OFTS and MFTS, respectively; n=1..3